

A NODALLY BOUND-PRESERVING FINITE ELEMENT METHOD FOR HYPERBOLIC CONVECTION-REACTION PROBLEMS

BEN S. ASHBY, ABDALAZIZ HAMDAN, AND TRISTAN PRYER

ABSTRACT. In this article, we present a numerical approach to ensure the preservation of physical bounds on the solutions to linear and nonlinear hyperbolic convection-reaction problems at the discrete level. We provide a rigorous framework for error analysis, formulating the discrete problem as a variational inequality and demonstrate optimal convergence rates in a natural norm. We summarise extensive numerical experiments validating the effectiveness of the proposed methods in preserving physical bounds and preventing unphysical oscillations, even in challenging scenarios involving highly nonlinear reaction terms.

1. INTRODUCTION

Ensuring that numerical approximations respect certain physical bounds presents a significant challenge across various fields in computational modelling. Many important PDE models rely on solutions that adhere to these bounds to maintain physical validity. For instance, in phase-field modelling, solutions must strictly preserve global maxima and minima [WGZ22], while in incompressible flow simulations, the velocity field is required to remain divergence-free [SL18]. Similarly, in applications such as kinetic equations, dose deposition modelling for external beam radiotherapy [ACH⁺24], or nuclear engineering [CEL⁺24], maintaining physical accuracy is critical to ensure reliable and safe operations, particularly when computational constraints limit the achievable numerical fidelity. These bounds, derived from fundamental physical principles, become especially important when the solution serves as input to subsequent models, where unphysical values could propagate errors and lead to erroneous predictions downstream.

A common manifestation of the failure of numerical solutions to satisfy these bounds is the oscillation of the solution around layers or irregularities in the PDE solution. For example, singularly perturbed elliptic problems often exhibit boundary layers, while hyperbolic problems can support discontinuities, which can lead to under- and over-shoots numerically (see §6). Even many stabilised numerical methods can exhibit unphysical oscillations that overshoot these maxima and minima, as illustrated in Figure 3b.

The aim of the method presented in this work is to prevent spurious numerical behaviour from violating maximum principles. We propose a finite element method that enforces physical bounds at nodal points by discretising the problem as a variational inequality. This ensures that the solution lies within a finite-dimensional, closed and convex subset of the natural solution space for the PDE. We provide bounds on the approximation error of the proposed bound-preserving finite element method, demonstrating optimal convergence rates for a scalar hyperbolic equation. This formulation enables rigorous error analysis and yields a simple implementation whilst also offering flexibility in computational mesh selection. Our analysis focusses on convection-reaction equations, a class of problems where bound preservation is particularly important due to the challenges posed by sharp gradients, boundary layers and discontinuities. Moreover, we extend our approach to nonlinear problems, leveraging appropriate quasi-norms to establish best-approximation results within the framework of variational formulations.

Standard finite element methods often fail to respect physical bounds without imposing additional constraints or modifications. For example, the most popular finite element methods for incompressible flows often fail to ensure pointwise divergence-free solutions, and proving energy stability in dissipative systems is similarly challenging (see, e.g., [GMP14, CJ21]). This was formalised early on in [CR73], which demonstrated that piecewise linear finite elements respect such bounds only under specific mesh conditions.

A variety of methods have been proposed to address these challenges. A notable approach is the development of methods satisfying the *Discrete Maximum Principle (DMP)*, particularly for convection-dominated convection-diffusion problems (see [MH85, XZ99, BE05, Kuz07, BJK17, BJK23, WY24], among others). These methods often involve nonlinear stabilisation, where additional nonlinear terms are introduced to

ensure that the discrete solution does not violate the maximum principle. Despite their effectiveness, these methods frequently rely on piecewise linear elements and extending them to higher-order elements introduces stricter mesh conditions and additional analytical complexities.

Related approaches include nodally bound-preserving stabilised methods [BGPV24, ABP24, BPT24], where the discrete solution is shown to satisfy a variational inequality. The idea of enforcing bounds by formulating the problem as a variational inequality has also appeared in [CN17, KS24b, KS24a]. These methods often involve solving nonlinear problems, a necessity highlighted by the Godunov barrier theorem, which asserts that achieving high-order accuracy while preserving monotonicity or bounds is generally impossible with linear methods. Consequently, nonlinearity is an inherent feature of any method aiming to respect maximum principles whilst retaining higher-order accuracy.

The rest of the paper is structured as follows: In §2 we introduce a model hyperbolic problem and discuss its solution, regularity and approximation by the finite element method. We then conduct an error analysis in §3. Following in §4, we provide a best approximation result for a hyperbolic problem with singular nonlinearity in the reaction term. Implementation details including methods to obtain an approximation to the finite element solution are given in §5. Finally, numerical experiments are presented in §6.

2. PROBLEM FORMULATION & DISCRETISATION

In what follows, $\Omega \subseteq \mathbb{R}^d$, $d = 2, 3$, is assumed to be a Lipschitz domain, ensuring that a unit outward normal vector \mathbf{n} is defined almost everywhere on $\partial\Omega$. For any measurable subset $\omega \subseteq \Omega$, let $L^p(\omega)$ denote the space of p -th power (Lebesgue) integrable functions over ω , equipped with the norm $\|\cdot\|_{L^p(\omega)}$. The L^2 inner product over ω is written as $\langle u, v \rangle_\omega := \int_\omega uv \, dx$, with the convention that the subscript is omitted if $\omega = \Omega$.

The standard Sobolev space $W^{k,p}(\omega)$ is defined as the space of functions in $L^p(\omega)$ whose weak derivatives of order at most k are also in $L^p(\omega)$. As is customary, $W^{k,2}(\omega)$ is denoted by $H^k(\omega)$.

For $\mathbf{b} : \Omega \rightarrow \mathbb{R}^d$ and $c : \Omega \rightarrow \mathbb{R}$, we introduce the linear hyperbolic problem given by

$$(1) \quad \begin{aligned} \mathbf{b} \cdot \nabla u + cu &= f && \text{in } \Omega \\ u &= g && \text{on } \Gamma_-, \end{aligned}$$

where Γ_- is the inflow boundary defined by the flow field \mathbf{b} , that is,

$$\Gamma_- = \{\mathbf{x} \in \partial\Omega : \mathbf{b}(\mathbf{x}) \cdot \mathbf{n}(\mathbf{x}) < 0\},$$

and

$$(2) \quad \Gamma_+ = \partial\Omega \setminus \Gamma_-.$$

The analysis of this linear problem is significantly more complicated than for advection-diffusion-reaction problems, as the smoothing properties enjoyed by elliptic operators are not present here. For example, even when \mathbf{b} is smooth, discontinuities can propagate along streamlines, leading to solutions which are quite irregular. We elaborate further on this point in Remark 2.2.

We now proceed to discuss questions of existence, uniqueness and regularity of solutions to (1). Let $\mathbf{b} \in C^1(\bar{\Omega})$ and $c \in C^0(\bar{\Omega})$ and suppose there exists $\mu > 0$ such that

$$(3) \quad c(x) - \frac{1}{2} \nabla \cdot \mathbf{b}(\mathbf{x}) \geq \mu \text{ for almost every } \mathbf{x} \in \Omega.$$

We define the function space

$$(4) \quad H_-(\Omega) = \{v \in L^2(\Omega) : \mathbf{b} \cdot \nabla v + cv \in L^2(\Omega), (\mathbf{b} \cdot \mathbf{n})v = 0 \text{ on } \Gamma_-\},$$

where boundary values are interpreted in the trace sense. We refer to [SP22, §3.1] for a justification of sufficient boundary regularity so that the boundary condition included in this definition is meaningful. The space $H_-(\Omega)$ is a Hilbert space when equipped with norm

$$(5) \quad \|v\|_{H_-(\Omega)}^2 = \|v\|_{L^2(\Omega)}^2 + \|\mathbf{b} \cdot \nabla v + cv\|_{L^2(\Omega)}^2,$$

allowing us to give the variational formulation of problem (1): find $u \in H_-(\Omega)$ such that

$$(6) \quad a(u, v) = l(v) \quad \forall v \in L^2(\Omega),$$

where

$$(7) \quad a(w, v) = \int_{\Omega} (\mathbf{b} \cdot \nabla w + cw) v,$$

and

$$(8) \quad l(v) = \int_{\Omega} f v.$$

The following result derived from Green's formula will be frequently used, and is stated here for convenience.

$$(9) \quad \int_{\Omega} (\mathbf{b} \cdot \nabla v) w = \int_{\partial\Omega} v w (\mathbf{b} \cdot \mathbf{n}) - \int_{\Omega} v (\mathbf{b} \cdot \nabla w) - \int_{\Omega} v w \operatorname{div}(\mathbf{b}).$$

We now present the main existence result, which assumes 'good' behaviour of the advection field \mathbf{b}

Proposition 2.1 (Existence & uniqueness of solutions [SP22]). *Suppose that Ω is a Lipschitz domain, and assume that the vector field \mathbf{b} lies in $C^1(\bar{\Omega})$, with all vector components strictly positive. We additionally assume $c \in C(\bar{\Omega})$. We assume additionally that g can be extended to Ω such that the result lies in $H_-(\Omega)$. For $f \in L^2(\Omega)$, there exists a unique solution $u \in H_-(\Omega)$ to problem (6).*

Remark 2.2 (Further remarks on regularity). *The conditions for the solution to problem (6) to have full $H^1(\Omega)$ -regularity are strong, requiring $f \in H_0^1(\Omega)$ in addition to higher regularity on \mathbf{b} (see [Rau72]). However, in special cases, less regular solutions can still be shown to exist. For example, as discussed in [HGR08, Part III, 1.1], in the special case where Ω is the unit square and the components of \mathbf{b} are bounded away from zero, there is a unique solution that lies in $H_-(\Omega)$ even when $g \in L^2(\Gamma_-)$, meaning problem (1) supports discontinuous solutions.*

More generally, as shown in [HGR08, Theorem 3.1], the problem admits a unique solution in $H_-(\Omega)$ provided g has an extension in $H_-(\Omega) \cap L^q(\Omega)$ for some $q \geq 2$. Similar results on the regularity of solutions can be found in [SP22, Ber12, GT10].

Of course, the numerical analysis of such cases is complicated by this lack of regularity. Indeed, it is precisely in these scenarios-where the boundary data or the solution exhibits low regularity-that spurious behaviour is frequently observed upon discretisation with many numerical methods.

Remark 2.3 (Problems satisfying a priori bounds). *For some choices of \mathbf{b} , problem (1) can be solved analytically using the method of characteristics. One such case is when \mathbf{b} has well-defined, non-intersecting streamlines with no stationary points. These conditions ensure that any $\mathbf{x} \in \Omega$ lies on a single characteristic curve which originates at the inflow boundary, and therefore u is the solution of an ODE along this characteristic with initial data given by the inflow boundary condition. Assuming further that $c \geq 0$ and that the boundary data $g \in L^\infty(\Gamma_-)$, we have for example that if $f = 0$ almost everywhere,*

$$(10) \quad u(\mathbf{x}) \leq \|g\|_{L^\infty(\Gamma_-)}.$$

2.1. Finite element discretisation. Let u be the solution of (6) and, without loss of generality, we assume that u satisfies the bound $u(\mathbf{x}) \in [0, 1]$ for almost every $\mathbf{x} \in \Omega$. We assume that the domain Ω is subdivided into a conforming, shape-regular triangulation \mathcal{T} , namely, \mathcal{T} is a finite family of sets such that

- (1) $K \in \mathcal{T}$ implies K is an open simplex or box,
- (2) for any $K, J \in \mathcal{T}$ we have that $\bar{K} \cap \bar{J}$ is a full lower-dimensional simplex (i.e., it is either \emptyset , a vertex, an edge or the whole of \bar{K} and \bar{J}) of both \bar{K} and \bar{J} and
- (3) $\bigcup_{K \in \mathcal{T}} \bar{K} = \bar{\Omega}$.

We additionally assume that the elements align with transitions between inflow and outflow boundaries. The finite element space \mathbb{V} is defined to be

$$(11) \quad \mathbb{V} := \{v_h \in C^0(\Omega) : v_h|_K \in \mathcal{R}(K) \ \forall K \in \mathcal{T}, v_h = 0 \text{ on } \Gamma_-\},$$

where $\mathcal{R}(K)$ is either $\mathbb{P}_k(K)$, the space of polynomials of degree k , or $\mathbb{Q}_k(K)$, the space of polynomials of total degree k , depending upon the triangulation. For an element $K \in \mathcal{T}$, we denote the diameter of K by h_K , with $h := \max_{K \in \mathcal{T}} h_K$. Finally, let $\mathbf{x}_1, \dots, \mathbf{x}_N$ be the union of the set of interior degrees of freedom and those that lie on the outflow boundary.

We define the convex subset K_h of \mathbb{V} by restricting the nodal values of function in \mathbb{V} , that is

$$(12) \quad K_h := \{v_h \in \mathbb{V} : v_h(\mathbf{x}_i) \in [0, 1], i = 1, \dots, N\}.$$

Remark 2.4 (Preservation of the bound at the degrees of freedom). *For polynomial degree, $k = 1$, the space K_h consists of precisely the finite element functions which satisfy the upper and lower bound pointwise since between nodes the functions are (bi)linearly interpolated. For polynomial degree, $k = 2$, or higher, this is not the case, and K_h is the set of finite element functions which are nodally bound preserving. This property was investigated in [BGPV24] for second order elliptic problems, where the authors obtain their approximations via a nonlinear stabilised method rather than a variational inequality. There, the bound preserving approximation was shown to be equivalent to the solution of a discrete variational inequality.*

Let δ_K , $K \in \mathcal{T}$, be positive real numbers and let a_h denote the bilinear form associated with the SUPG stabilisation method [BH82, JNP84], defined as

$$(13) \quad a_h(w_h, v_h) = \int_{\Omega} (\mathbf{b} \cdot \nabla w_h + c v_h) v_h + \sum_{K \in \mathcal{T}} \delta_K \int_K (\mathbf{b} \cdot \nabla w_h + c w_h) \mathbf{b} \cdot \nabla v_h.$$

The numbers δ_K are the SUPG parameters which determine the local degree of stabilisation. The bilinear form a_h has an associated norm for $w \in \mathbb{H}_-$

$$(14) \quad \|w\|^2 := \mu \|w\|_{L^2(\Omega)}^2 + \sum_{K \in \mathcal{T}} \left\| \delta_K^{\frac{1}{2}} \mathbf{b} \cdot \nabla w \right\|_{L^2(K)}^2 + |w|_{\Gamma^+}^2,$$

where

$$|w|_{\Gamma^+}^2 := \int_{\Gamma^+} (\mathbf{b} \cdot \mathbf{n}) w^2.$$

Then the finite element discretisation is to find $u_h \in K_h$ such that

$$(15) \quad a_h(u_h, v_h - u_h) \geq l_h(v_h - u_h) \quad \forall v_h \in K_h,$$

where

$$l_h(v_h) := \int_{\Omega} f v_h + \sum_{K \in \mathcal{T}} \delta_K \int_K f (\mathbf{b} \cdot \nabla v_h).$$

3. ERROR ANALYSIS

In this section we prove the main result of this work: an error bound for $\|u - u_h\|$, where u_h is a bound-preserving approximation to $u \in \mathbb{H}_-(\Omega)$. The key idea is that we can combine the weak forms of the variational problem (6) and the discrete inequality (15) and use the coercivity and continuity of a_h and the consistency of the SUPG formulation to derive a best approximation result. Consistency is the subject of the next lemma.

Lemma 3.1 (Consistency of the SUPG method). *Let u be the solution of problem (6). Then for any $v_h \in \mathbb{V}$,*

$$l_h(v_h) - a_h(u, v_h) = 0.$$

Proof. Note that

$$(16) \quad \begin{aligned} a_h(u, v_h) &= \int_{\Omega} (\mathbf{b} \cdot \nabla u + c u) v_h + \sum_{K \in \mathcal{T}} \delta_K \int_K (\mathbf{b} \cdot \nabla u + c u) \mathbf{b} \cdot \nabla v_h \\ &= \int_{\Omega} f v_h + \sum_{K \in \mathcal{T}} \delta_K \int_K f \mathbf{b} \cdot \nabla v_h = l_h(v_h), \end{aligned}$$

by (6). □

Lemma 3.2 (Continuity & coercivity properties of a_h). *Assume that, for all $K \in \mathcal{T}$, the SUPG parameters δ_K are chosen so that*

$$(17) \quad 0 \leq \delta_K \leq \frac{\mu}{\|c\|_{L^\infty(K)}^2}.$$

Then the bilinear form a_h is coercive over H_- with respect to the norm $\|\cdot\|$, that is, for $w \in H_-$

$$(18) \quad a_h(w, w) \geq \frac{1}{2} \|w\|^2.$$

Furthermore, for $w \in H_-$ we define the norm

$$(19) \quad \|w\|_*^2 := \|w\|^2 + \sum_{K \in \mathcal{T}} \delta_K^{-1} \|w\|_{L^2(K)}^2.$$

Then, for $w, v \in H_-$ a_h satisfies the continuity result

$$(20) \quad a_h(w, v) \leq C \|w\|_* \|v\|.$$

Proof. We first show coercivity. Using (9) yields

$$(21) \quad a_h(w, w) \geq \inf_{x \in \Omega} \left(c - \frac{1}{2} \nabla \cdot \mathbf{b} \right) \|w\|_{L^2(\Omega)}^2 + \frac{1}{2} \int_{\partial\Omega} (\mathbf{b} \cdot \mathbf{n}) |w|^2 + \sum_{K \in \mathcal{T}} \left\| \delta_K^{\frac{1}{2}} \mathbf{b} \cdot \nabla w \right\|_{L^2(K)}^2 - \left| \sum_{K \in \mathcal{T}} \delta_K \int_K cw(\mathbf{b} \cdot \nabla w) \right|,$$

where only the final term on the right hand side remains to be estimated. To this end, we observe that, on any $K \in \mathcal{T}$,

$$(22) \quad \left| \int_K \delta_K cw(\mathbf{b} \cdot \nabla w) \right| \leq \delta_K^{\frac{1}{2}} \|c\|_{L^\infty(K)} \|w\|_{L^2(K)} \left\| \delta_K^{\frac{1}{2}} \mathbf{b} \cdot \nabla w \right\|_{L^2(K)}.$$

We now split this product using Young's inequality and note the choice of δ_K , given in (17) to see that

$$(23) \quad \left| \int_K \delta_K cw(\mathbf{b} \cdot \nabla w) \right| \leq \frac{1}{2} \delta_K \|c\|_{L^\infty(K)}^2 \|w\|_{L^2(K)}^2 + \frac{1}{2} \left\| \delta_K^{\frac{1}{2}} \mathbf{b} \cdot \nabla w \right\|_{L^2(K)}^2 \leq \frac{1}{2} \mu \|w\|_{L^2(K)}^2 + \frac{1}{2} \left\| \delta_K^{\frac{1}{2}} \mathbf{b} \cdot \nabla w \right\|_{L^2(K)}^2,$$

from which the result follows. To show continuity, we again use Green's formula and bound

$$(24) \quad \begin{aligned} a_h(w, v) &= \int_{\Omega} (\mathbf{b} \cdot \nabla w + cw) v + \sum_{K \in \mathcal{T}} \delta_K \int_K (\mathbf{b} \cdot \nabla w + cw) \mathbf{b} \cdot \nabla v \\ &= \int_{\Omega} (c - \operatorname{div} \mathbf{b}) wv - \int_{\Omega} (\mathbf{b} \cdot \nabla v) w + \int_{\partial\Omega} (\mathbf{b} \cdot \mathbf{n}) wv \\ &\quad + \sum_{K \in \mathcal{T}} \int_K \left(\delta_K^{\frac{1}{2}} \mathbf{b} \cdot \nabla w \right) \left(\delta_K^{\frac{1}{2}} \mathbf{b} \cdot \nabla v \right) + \sum_{K \in \mathcal{T}} \delta_K \int_K cw(\mathbf{b} \cdot \nabla v). \end{aligned}$$

An application of Cauchy-Schwarz results in

$$(25) \quad \begin{aligned} |a_h(w, v)| &\leq \|c - \operatorname{div} \mathbf{b}\|_{L^\infty(\Omega)} \|w\|_{L^2(\Omega)} \|v\|_{L^2(\Omega)} + \sum_{K \in \mathcal{T}} \left\| \delta_K^{\frac{1}{2}} \mathbf{b} \cdot \nabla w \right\|_{L^2(K)} \left\| \delta_K^{-\frac{1}{2}} w \right\|_{L^2(K)} \\ &\quad + |w|_{\Gamma_+} |v|_{\Gamma_+} + \sum_{K \in \mathcal{T}} \left\| \delta_K^{\frac{1}{2}} \mathbf{b} \cdot \nabla w \right\|_{L^2(K)} \left\| \delta_K^{\frac{1}{2}} \mathbf{b} \cdot \nabla v \right\|_{L^2(K)} \\ &\quad + \sum_{K \in \mathcal{T}} \|c\|_{L^\infty(K)} \delta_K^{\frac{1}{2}} \|w\|_{L^2(K)} \left\| \delta_K^{\frac{1}{2}} \mathbf{b} \cdot \nabla v \right\|_{L^2(K)}. \end{aligned}$$

Finally, let $M = \max \left\{ 1, \|c - \operatorname{div} \mathbf{b}\|_{L^\infty(\Omega)}, \|c\|_{L^\infty(\Omega)} \max_K \delta_K^{1/2} \right\}$. Then applying a discrete Cauchy-Schwarz inequality to (25) gives

$$(26) \quad |a_h(w, v)| \leq 2 \frac{M}{\mu} \|w\|_* \|v\|,$$

as required. \square

Theorem 3.3 (Best approximation). *Let $u \in H_-(\Omega)$ be the solution of (6) and let $u_h \in K_h$ be the solution of (15). Then we have the following best approximation result:*

$$\|u - u_h\| \leq C \inf_{v_h \in K_h} \|u - v_h\|_*.$$

Proof. We begin our estimation noting that, by coercivity of a_h with respect to the norm $\|\cdot\|$,

$$(27) \quad \frac{1}{2} \|u - u_h\|^2 \leq a_h(u - u_h, u - u_h).$$

By consistency, shown in Lemma 3.1, we have

$$(28) \quad a_h(u, u_h - v_h) = l_h(u_h - v_h),$$

and since u_h satisfies the discrete problem (15) we have

$$(29) \quad a_h(u_h, u_h - v_h) \leq l_h(u_h - v_h).$$

Equations (28) and (29) together imply that

$$a_h(u - u_h, u_h - v_h) \geq 0.$$

The inequality (27) therefore leads to

$$\frac{1}{2} \|u - u_h\|^2 \leq a_h(u - u_h, u - v_h) \leq 2 \frac{M}{\mu} \|u - v_h\|_* \|v_h - u_h\|,$$

where we have used the continuity result (20), concluding the proof. \square

Remark 3.4 (Relation to Falk's estimate [Fal74]). *In the context of finite element approximations for variational inequalities, the equality stated in Lemma 3.1 does not generally hold. Instead, approximation results typically involve additional terms arising from the projection of the exact solution onto a cone, as discussed in [BHR77, Theorem 2.1]. However, in our setting, the exact solution is not projected onto a cone, whereas the discretisation is. This distinction eliminates certain terms that would otherwise appear on the right-hand side of the analogous error bound for elliptic variational inequalities.*

Corollary 3.5 (Rates of convergence). *Let $\mathbf{b} \in W^{1,\infty}(\Omega)$, $c \in L^\infty(\Omega)$, and let u be the unique solution of (6), with $u_h \in K_h$ the solution of (15). Let $k \geq 1$, and assume that $u \in H^r(\Omega)$, where $r > \frac{d}{2}$ is sufficiently large so that u is regular enough to belong to the domain of the Lagrange interpolation operator. Suppose that $C_\delta > 0$ is sufficiently small so that*

$$\delta_K := C_\delta h_K \leq \frac{\mu}{\|c\|_{L^\infty(K)}^2}.$$

Then, there exists a constant $C > 0$ independent of h such that

$$(30) \quad \|u - u_h\| \leq C h^{\min\{k+1, r\} - \frac{1}{2}} |u|_{H^r(\Omega)}.$$

Proof. Since $u(x) \in [0, 1]$ for all x , the piecewise polynomial Lagrange interpolant of u , $\mathcal{I}u$ onto the finite element space associated with any sufficiently regular triangulation of Ω also has $\mathcal{I}u(x_i) \in [0, 1]$, $i = 1, \dots, N$. We therefore have $\mathcal{I}u \in K_h$ and therefore we can take $v_h = \mathcal{I}u$ in Theorem 3.3 and apply standard interpolation estimates [EG21] to the terms in the $\|\cdot\|_*$ norm. With $C_{\mathcal{I}}$ and C_{tr} the constants in the interpolation and trace estimates respectively, one sees that

$$(31) \quad \|u - \mathcal{I}u\|_{L^2(\Omega)} \leq C_{\mathcal{I}} h^r |u|_{H^r(\Omega)},$$

$$(32) \quad \left\| \delta_K^{\frac{1}{2}} \mathbf{b} \cdot \nabla (u - \mathcal{I}u) \right\|_{L^2(K)} \leq C_{\mathcal{I}} \|\mathbf{b}\|_{L^\infty(K)} C_\delta^{\frac{1}{2}} h^{r - \frac{1}{2}} |u|_{H^r(\Omega)},$$

$$(33) \quad \delta_K^{-\frac{1}{2}} \|u - \mathcal{I}u\|_{L^2(K)} \leq C_{\mathcal{I}} C_\delta^{-\frac{1}{2}} h^{r - \frac{1}{2}} |u|_{H^r(\Omega)}.$$

For the boundary norm, we appeal to a trace estimate, followed by estimates for the Lagrange interpolation error:

$$(34) \quad \begin{aligned} |u - \mathcal{I}u|_{\Gamma \cap K} &\leq C_{\text{tr}} \left(h_K^{-\frac{1}{2}} \|u - \mathcal{I}u\|_{L^2(K)} + h_K^{\frac{1}{2}} \|\nabla(u - \mathcal{I}u)\|_{L^2(K)} \right) \\ &\leq 2C_{\text{tr}} C_{\mathcal{I}} h_K^{r-\frac{1}{2}} |u|_{\mathbb{H}^r(\Omega)}. \end{aligned}$$

After collecting Equations (31)-(34), the result follows. \square

4. EXTENSION TO THE CASE OF NONLINEAR REACTION

We now consider the extension of the analysis of the previous sections to the problem

$$(35) \quad \begin{aligned} \mathbf{b} \cdot \nabla u + |u|^{p-2} u &= f \quad \text{in } \Omega \\ u &= 0 \quad \text{on } \Gamma_-, \end{aligned}$$

where $1 < p \leq 2$. The problem therefore has nonlinear reaction which is singular as $u \rightarrow 0$, meaning that preservation of positivity of solutions becomes very important.

Define (cf. Equation (4))

$$\mathbb{H}_{-,p}(\Omega) = \{v \in L^2(\Omega) : \mathbf{b} \cdot \nabla v + |v|^{p-2} v \in L^2(\Omega), (\mathbf{b} \cdot \mathbf{n})v = 0 \text{ on } \Gamma_-\}.$$

Then the weak form of problem (35) is to find $u \in \mathbb{H}_{-,p}(\Omega)$ such that

$$(36) \quad a(u, v) + b(u; u, v) = l(v) \quad \forall v \in L^2(\Omega),$$

where $a(\cdot, \cdot)$ and $l(\cdot)$ are as defined in (7) and (8) (the former with $c \equiv 0$), and where the semilinear form b is defined to be

$$(37) \quad b(u; v, w) = \int_{\Omega} |u|^{p-2} v w \, dx.$$

Remark 4.1 (Existence and uniqueness). *The existence and uniqueness of solutions to this problem, in the presence of diffusion, can be established using monotone operator theory, as detailed in [RR06, Chapter 10]. While the proof techniques for the corresponding linear problem do not straightforwardly generalise to the nonlinear case, they can be adapted through fixed-point arguments.*

Classical error analysis in the $L^p(\Omega)$ norm often leads to suboptimal estimates for $p \neq 2$. To address this issue, quasi-norms were introduced in [BL93] as a tool for achieving optimal convergence rates. We define the following quasi-norm, for fixed $w \in L^p(\Omega)$, we let

$$(38) \quad \|v\|_{(w,p)}^2 := \int_{\Omega} |v|^2 (|v| + |w|)^{p-2} \, dx,$$

for all $v \in L^p(\Omega)$.

4.1. Preliminary results. Error analysis in quasi-norms requires technical lemmata which are stated here for convenience. The key results are strong monotonicity and boundedness properties of the form b with respect to the quasi-norm, given in Lemma 4.3 and Lemma 4.4 respectively.

Lemma 4.2. ([BL93, Lemma 2.1]). *Let $p > 1$ and $x, y \in \mathbb{R}$. Then there exist positive constants C_1, C_2 depending only upon p such that*

$$(39) \quad ||x|^{p-2} x - |y|^{p-2} y| \leq C_1 (|x| + |y|)^{p-2} |x - y|,$$

$$(40) \quad (|x|^{p-2} x - |y|^{p-2} y) (x - y) \geq C_2 (|x| + |y|)^{p-2} |x - y|^2,$$

Lemma 4.3. *There exists $C_C > 0$ such that, for all $u, v \in L^p(\Omega)$,*

$$(41) \quad b(u; u, u - v) - b(v; v, u - v) \geq C_C \|u - v\|_{(u,p)}^2.$$

Proof. We first note that

$$(42) \quad |x| + |y| = |x| + |y - x + x| \leq 2|x| + |x - y|,$$

We therefore we have, noting that $p < 2$,

$$(43) \quad \begin{aligned} (|x|^{p-2}x - |y|^{p-2}y)(x - y) &\geq C_2 (|x| + |y|)^{p-2} |x - y|^2 \\ &\geq 2^{p-2}C_2 (|x| + |x - y|)^{p-2} |x - y|^2, \end{aligned}$$

and so the result follows with $C_C = 2^{p-2}C_2$. \square

Lemma 4.4. *For $1 < p < 2$, there exists $C_B > 0$ such that for any $\theta \in (0, 1]$ and any $u, v, w \in L^p(\Omega)$,*

$$(44) \quad |b(u; u, w) - b(v; v, w)| \leq C_B \left(\theta \|u - v\|_{(u,p)}^2 + \theta^{-1} \|w\|_{(u,p)}^2 \right).$$

Proof. For real numbers x, y and z , we apply (39) to see that

$$(45) \quad \begin{aligned} \left| |x|^{p-2}x - |y|^{p-2}y \right| |w| &\leq C_1 (|x| + |y|)^{p-2} |x - y| |w| \\ &\leq C'_1 (|x| + |x - y|)^{p-2} |x - y| |w|, \end{aligned}$$

which can be further bounded by invoking [Liu00, Lemma 2.2] with $a = |x|, \sigma_1 = |x - y|, \sigma_2 = |z|, \alpha = 1$ and $r = p$. This gives the bound

$$(46) \quad \left| |x|^{p-2}x - |y|^{p-2}y \right| |z| \leq C_B \left(\theta (|x| + |x - y|)^{p-2} |x - y|^2 + \theta^{-1} (|x| + |z|)^{p-2} |z|^2 \right),$$

from which the desired result is immediate. \square

4.2. Finite element discretisation. We present the finite element method for the nonlinear problem as an extension of the linear case by treating the advection with SUPG-stabilisation. The discrete problem is then to find $u_h \in K_h$ such that

$$(47) \quad a_h(u_h, v_h - u_h) + b(u_h; u_h, v_h - u_h) \geq l_h(v_h - u_h) \quad \forall v_h \in K_h,$$

where a_h is as defined in Equation (13) with $c \equiv 0$ and b is the semilinear form defined in Equation (37).

Remark 4.5 (Weaker control of the advective term). *In the following analysis, we prove a best approximation result by treating the advective part in an analogous way to Theorem 3.3, and the nonlinear part separately with the quasi-norm $\|\cdot\|_{(u,p)}$. Since we are then working with the SUPG bilinear form a_h with the reaction coefficient c set to be identically zero, we can no longer assume the coercivity condition (3). As a result, the coercivity shown in Lemma 3.2 is replaced with the weaker notion*

$$(48) \quad a_h(v_h, v_h) = |v_h|_{\Gamma_+}^2 + \sum_{K \in \mathcal{T}} \left\| \delta_K^{\frac{1}{2}} \mathbf{b} \cdot \nabla v_h \right\|_{L^2(K)}^2.$$

We therefore note that control of the error in $L^2(\Omega)$ is lost, or rather replaced, with error control in $\|\cdot\|_{(u,p)}$.

The weak norm given on the right hand side of Equation (48) is the norm $\|\cdot\|$ (cf. Equation (14)) with μ set to zero. For the remainder of this section we will reuse $\|\cdot\|$ to denote this weaker norm, and adopt a similar convention for $\|\cdot\|_*$.

Lemma 4.6 (Quantification of inconsistency (cf. Lemma 3.1)). *Let u be the solution to problem 36. Then for any $w_h \in \mathbb{V}$,*

$$(49) \quad l_h(w_h) - a_h(u, w_h) - b(u; u, w_h) = \sum_{K \in \mathcal{T}} \delta_K \int_K |u|^{p-2} u (\mathbf{b} \cdot \nabla w_h).$$

Proof. The result follows after evaluating the left hand side of Equation 49 to obtain

$$(50) \quad \int_{\Omega} (f - \mathbf{b} \cdot \nabla u - |u|^{p-2}u) w_h + \sum_{K \in \mathcal{T}} \delta_K \int_K (f - \mathbf{b} \cdot \nabla u) (\mathbf{b} \cdot \nabla w_h),$$

and using the fact that u is the solution of Equation 35. \square

Theorem 4.7 (Best approximation). *Assume that $\operatorname{div} \mathbf{b} = 0$, that u is the solution of (36), and that u_h is the finite element solution, that is, the solution of (47). Then*

$$(51) \quad \begin{aligned} \|u - u_h\|^2 + \|u - u_h\|_{(u,p)}^2 &\leq C \inf_{v_h \in K_h} \left(\|u - v_h\|_{(u,p)}^2 + \|u - v_h\|_*^2 \right) \\ &\quad + \sup_{0 \neq w_h \in \mathbb{V}} \frac{\sum_{K \in \mathcal{T}} \delta_K \int_K |u|^{p-2} u (\mathbf{b} \cdot \nabla w_h)}{\|w_h\|}. \end{aligned}$$

Proof. From the coercivity result (41), and in light of Equation (48), we immediately have

$$(52) \quad \|u - u_h\|^2 + C_C \|u - u_h\|_{(u,p)}^2 \leq a_h(u - u_h, u - u_h) + b(u; u, u - u_h) - b(u_h; u_h, u - u_h).$$

We now wish to introduce an arbitrary v_h . To this end, invoking Lemma 4.6 with $w_h = u_h - v_h$, and using the fact that u_h satisfies Equation (47), we conclude that

$$(53) \quad \begin{aligned} a_h(u - u_h, u_h - v_h) + b(u; u, u_h - v_h) - b(u_h; u_h, u_h - v_h) \\ + \sum_{K \in \mathcal{T}} \delta_K \int_K |u|^{p-2} u (\mathbf{b} \cdot \nabla (u_h - v_h)) \geq 0. \end{aligned}$$

Then (cf. Theorem 3.3) we can write

$$(54) \quad \begin{aligned} a_h(u - u_h, u - u_h) + b(u; u, u - u_h) - b(u_h; u_h, u - u_h) \\ \leq a_h(u - u_h, u - v_h) + b(u; u, u - v_h) - b(u_h; u_h, u - v_h) \\ + \sum_{K \in \mathcal{T}} \delta_K \int_K |u|^{p-2} u (\mathbf{b} \cdot \nabla (u_h - v_h)). \end{aligned}$$

Using Lemma 4.4

$$(55) \quad b(u; u, u - v_h) - b(u_h; u_h, u - v_h) \leq C_B \left(\theta \|u - u_h\|_{(u,p)}^2 + \theta^{-1} \|u - v_h\|_{(u,p)}^2 \right).$$

We apply a boundedness argument analogous to Lemma 3.2 to see

$$(56) \quad a_h(u - u_h, u - v_h) \leq \|u - v_h\|_* \|u - u_h\| \leq \frac{1}{2} \|u - v_h\|_*^2 + \frac{1}{2} \|u - u_h\|^2.$$

Upon making the choice of $\theta = \min\left(\frac{C_C}{2C_B}, \frac{1}{2}\right)$, collecting Equations (52)-(56), we have

$$(57) \quad \|u - u_h\|^2 + \|u - u_h\|_{(u,p)}^2 \leq \|u - v_h\|_*^2 + \Theta \|u - v_h\|_{(u,p)}^2 + \sum_{K \in \mathcal{T}} \delta_K \int_K |u|^{p-2} u (\mathbf{b} \cdot \nabla (u_h - v_h)),$$

where $\Theta = \max\left(2\frac{C_B}{C_C}, 2\frac{C_B^2}{C_C^2}\right)$, concluding the proof. \square

5. OVERVIEW OF ACTIVE-SET TECHNIQUES AND APPLICATIONS

The variational inequality (15), posed over the finite-dimensional space K_h , is nonlinear and must be solved using an iterative method. In this section, we describe solution techniques for this class of problems. Throughout, we denote a vector $\boldsymbol{\xi} \in \mathbb{R}^N$ as non-negative, written $\boldsymbol{\xi} \geq 0$, if all its components satisfy $(\boldsymbol{\xi})_i \geq 0$.

The problem (15) can be viewed as a specific instance of the general variational inequality

$$(58) \quad \langle G(u), v - u \rangle \geq 0 \quad \forall v \in K,$$

where $G : V \rightarrow V$ is a mapping on a Banach space V and K is a closed and convex subset of V . In the discrete setting, we introduce a discrete operator $\bar{G}_h : \mathbb{V} \rightarrow \mathbb{V}$ and reformulate (15) as: find $u_h \in K_h$ such that:

$$(59) \quad \langle \bar{G}_h(u_h), v_h - u_h \rangle \geq 0 \quad \forall v_h \in K_h.$$

An equivalent reformulation involves a mapping $G_h : \mathbb{R}^N \rightarrow \mathbb{R}^N$, where N denotes the dimension of the finite element space. This mapping is defined using the finite element system matrix and right-hand side. Specifically, let \mathbf{A}_h represent the assembled system matrix such that

$$(60) \quad (\mathbf{A}_h)_{ij} = a_h(\varphi_j, \varphi_i),$$

with $\{\varphi_i\}_{i=1}^N$ the nodal basis functions. Similarly, let

$$(61) \quad (\mathbf{F}_h)_i = l_h(\varphi_i).$$

If $\mathbf{V} \in \mathbb{R}^N$ is the vector of degrees of freedom corresponding to a finite element function v_h , given by:

$$(62) \quad v_h(\mathbf{x}) = \sum_{i=1}^N \mathbf{V}_i \varphi_i(\mathbf{x}),$$

then the mapping $G_h : \mathbb{R}^N \rightarrow \mathbb{R}^N$ is given by:

$$(63) \quad G_h(\mathbf{V}) = \mathbf{A}_h \mathbf{V} - \mathbf{F}_h.$$

We also define the discrete set

$$(64) \quad K_{h,N} := \{\mathbf{V} \in \mathbb{R}^N : 0 \leq \mathbf{V}_i \leq 1, i = 1, \dots, N\}.$$

The discrete variational inequality (15) can now be reformulated algebraically as: Find $\mathbf{U} \in K_{h,N}$ such that

$$(65) \quad G_h(\mathbf{U}) \cdot (\mathbf{V} - \mathbf{U}) \geq 0 \quad \forall \mathbf{V} \in K_{h,N}.$$

Definition 5.1 (Projection Operators). *Let $P : \mathbb{V} \rightarrow K_h$ denote the orthogonal projection onto the closed convex subset K_h . Assuming K_h is a box as defined in (12), the projection P has a simple explicit form. For $v_h \in K_h$, we define:*

$$(66) \quad P(v_h) := \sum_{i=1}^N \max\{0, \min\{v_h(\mathbf{x}_i), 1\}\} \varphi_i.$$

Similarly, we define the projection in the Euclidean setting, $\Pi : \mathbb{R}^N \rightarrow K_{h,N}$, as:

$$(67) \quad \Pi(\mathbf{X})_i := \max\{0, \min\{\mathbf{X}_i, 1\}\}.$$

5.1. Projection Methods. For discretisations of many elliptic variational inequalities, a common approach combines iterative schemes, such as Richardson iteration or successive over-relaxation (SOR), with a projection step. These methods ensure that the iterates remain within the convex set and are relatively straightforward to implement. The underlying principle for such methods is that the discrete problem can often be reformulated as a minimisation problem, allowing the application of various well-established optimisation algorithms.

However, when the finite element system matrix is not symmetric, as is the case in this problem, these classical methods generally fail to converge. This limitation necessitates the use of projection methods that are robust under broader assumptions. One such method, introduced in [Alf94], iteratively projects the solution back onto the feasible set and is defined as follows. Given an initial guess $u_h^0 \in K_h$, the method updates the iterate using:

$$(68) \quad u_h^{j+1} = P\left(u_h^j - \gamma \bar{G}_h(u_h^j)\right),$$

where $\gamma > 0$ is a step size parameter. Iteration is terminated when the stopping criterion $\|u_h^{j+1} - u_h^j\| < \text{TOL}$ is satisfied, for a given tolerance TOL.

The projection method, as detailed in [Alf94], converges to a solution under the assumptions that the operator is monotone and Lipschitz continuous, without requiring differentiability. While this method is simple and guarantees convergence, it often requires many iterations to achieve acceptable accuracy. Consequently, for large-scale problems or those demanding high efficiency, more advanced and scalable methods are necessary to enhance convergence rates and reduce computational costs.

5.2. Reduced-Space Active Set Method. The numerical results presented in this work were obtained using the finite element discretisation package Firedrake [HKM⁺23], which leverages PETSc [BGMS98] for solving the variational inequalities introduced in Sections 2 and 4. Among the various solvers available in PETSc, we employed the reduced-space active-set method [BM06]. This method is particularly well-suited for parallel implementations and guarantees that the computed solution satisfies the imposed constraints. Although no formal convergence proofs were provided in [BM06], the method has demonstrated efficiency

and robustness in numerous test cases, especially in applications involving monotone operators, which aligns with the scope of this work.

Let $\mathbf{X} \in \mathbb{R}^N$. Define the active and inactive sets associated with \mathbf{X} as follows:

$$(69) \quad A_0(\mathbf{X}) := \{i : \mathbf{X}_i = 0 \text{ and } G_h(\mathbf{X})_i > 0\},$$

$$(70) \quad A_1(\mathbf{X}) := \{i : \mathbf{X}_i = 1 \text{ and } G_h(\mathbf{X})_i \leq 0\},$$

$$(71) \quad A(\mathbf{X}) := A_0(\mathbf{X}) \cup A_1(\mathbf{X}),$$

$$(72) \quad I(\mathbf{X}) := \{1, 2, \dots, N\} \setminus A(\mathbf{X}),$$

where $G_h(\mathbf{X})_i$ denotes the i^{th} component of the nonlinear residual evaluated at \mathbf{X} . The set $A(\mathbf{X})$ contains the indices of degrees of freedom where the box constraints are active, while $I(\mathbf{X})$ denotes the inactive set.

In the reduced-space active set method, starting from an initial guess \mathbf{X}^0 , the degrees of freedom corresponding to $A(\mathbf{X}^j)$ are fixed at each iteration. A linear system, derived from the linearisation of G_h , is solved over the inactive set $I(\mathbf{X}^j)$ to compute an update $\delta\mathbf{X}^j$, analogous to Newton's method. Specifically, let $G_h^I(\mathbf{X}^j)$ denote the reduced residual vector containing only the entries indexed by $I(\mathbf{X}^j)$, and let J^I be the Jacobian of G_h^I restricted to the inactive set. The update is then decomposed as

$$(73) \quad \delta\mathbf{X}^j = \delta^I \mathbf{X}^j \oplus \delta^A \mathbf{X}^j,$$

where $\delta^A \mathbf{X}^j = \mathbf{0}$, and $\delta^I \mathbf{X}^j$ satisfies

$$(74) \quad J^I \delta^I \mathbf{X}^j = -G_h^I(\mathbf{X}^j).$$

The updated solution is then computed as

$$(75) \quad \mathbf{X}^{j+1} = \Pi(\mathbf{X}^j + \alpha \delta\mathbf{X}^j),$$

where Π denotes the projection onto the constrained space $K_{h,N}$, as defined in (67). A line search is used to determine the step size α , employing either backtracking or a secant-based algorithm provided by PETSc. For further details on the selection of α , we refer the reader to [BM06, ZYK⁺21].

Importantly, due to the projection in (75), all iterates satisfy the box constraints, i.e., $\mathbf{X}^j \in K_{h,N}$ for all j . The algorithm terminates when either the residual or the relative reduction in the residual falls below a specified tolerance, set to 10^{-8} in this work.

6. NUMERICAL EXPERIMENTS

In this section, we present a summary of numerical experiments that validate the convergence rates predicted by the theoretical results of the previous sections. Additionally, we illustrate the effectiveness of the bound-preserving method in handling less smooth cases, where rigorous theoretical guarantees are unavailable.

6.1. Example 1: convergence to a smooth solution. We first examine a test case for which we expect the exact solution to possess higher regularity than functions in $H_-(\Omega)$ (cf. Remark 2.2). To this end, let $\Omega = (0, 1) \times (0, 1)$, and let $\mathbf{b}_1 = (1, \sqrt{2})$, so that the inflow boundary is

$$\Gamma^+ = \{(x, y) \in \partial\Omega : x = 0\} \cup \{(x, y) \in \partial\Omega : y = 0\}.$$

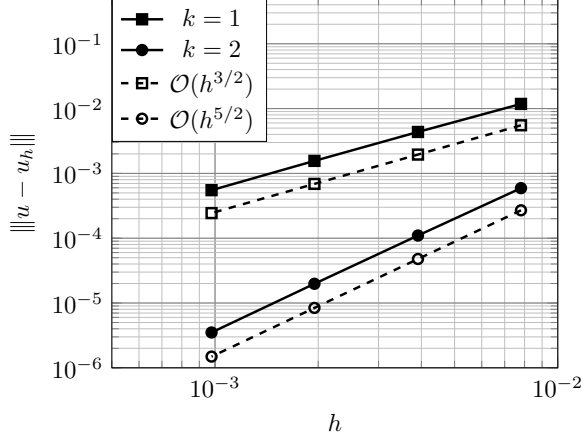
Smooth inflow boundary data is prescribed:

$$(76) \quad g_1(x, y) := \begin{cases} \exp\left(1 - \frac{1}{1-5(x-\frac{1}{2})^2}\right) & \text{if } |x - \frac{1}{2}| < \frac{1}{\sqrt{5}}, \\ 0 & \text{otherwise.} \end{cases}$$

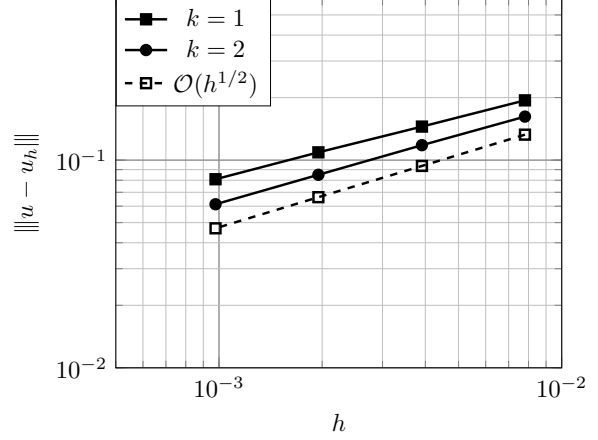
Finally, let $c \equiv 1$ and let the right hand side f be identically zero. Then an exact solution $u_1 \in C^\infty(\bar{\Omega})$ can be found using the method of characteristics. One finds that

$$(77) \quad u_1(x, y) = \begin{cases} g_1\left(x - \frac{y}{\sqrt{2}}, y\right) \exp\left(-\frac{y}{\sqrt{2}}\right) & \text{if } -\sqrt{\frac{2}{5}} < y - x\sqrt{2} + \frac{1}{\sqrt{2}} < \sqrt{\frac{2}{5}}, \\ 0 & \text{otherwise.} \end{cases}$$

Convergence results of the bound-preserving finite element method for piecewise linear and quadratic elements are shown in Figure 1a. In both cases the theoretical convergence rate of $k + \frac{1}{2}$ shown in Corollary

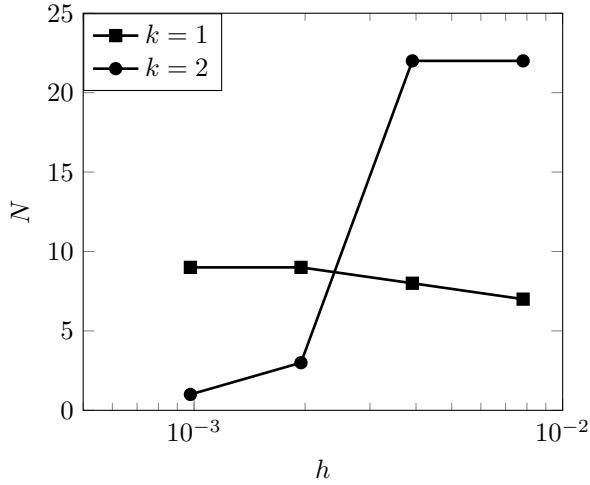


(A) Approximation error for Example 1, §6.1, smooth solution.

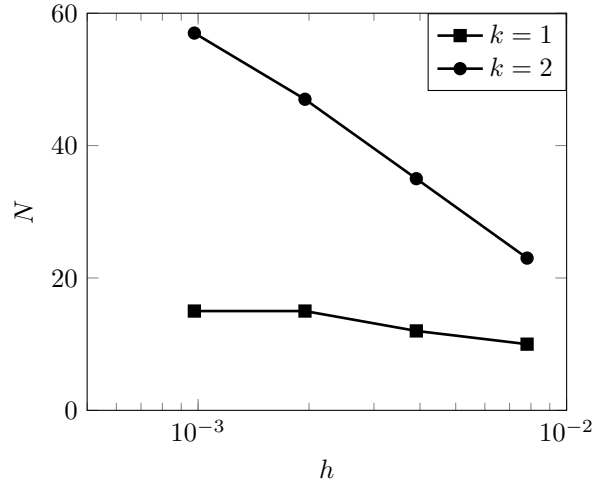


(B) Approximation error for Example 2, §6.2, solution in $H_-(\Omega) \setminus H^1(\Omega)$ only.

FIGURE 1. Approximation errors for the bound-preserving finite element method in the full SUPG norm $\|\cdot\|$. Polynomial degrees $k = 1, 2$ shown, yielding expected convergence rates of $3/2$ and $5/2$ respectively in the smooth case. As expected when the solution has minimal regularity, theoretical rates are not attained and there is no benefit to increasing polynomial degree.



(A) $u \in H^3(\Omega)$.



(B) $u \in H_-(\Omega) \setminus H^1(\Omega)$.

FIGURE 2. Active-set reduced-space iteration counts until the residuals or their relative reduction reach 10^{-8} . Note that for the smooth solution the number of iterations required is stable as the mesh is refined, while in the nonsmooth case number iterations increase.

3.5 is attained. The number of iterations required by the variational inequality solver is shown in Figure 2a. Note that with decreasing h the number required is either stable or decreasing.

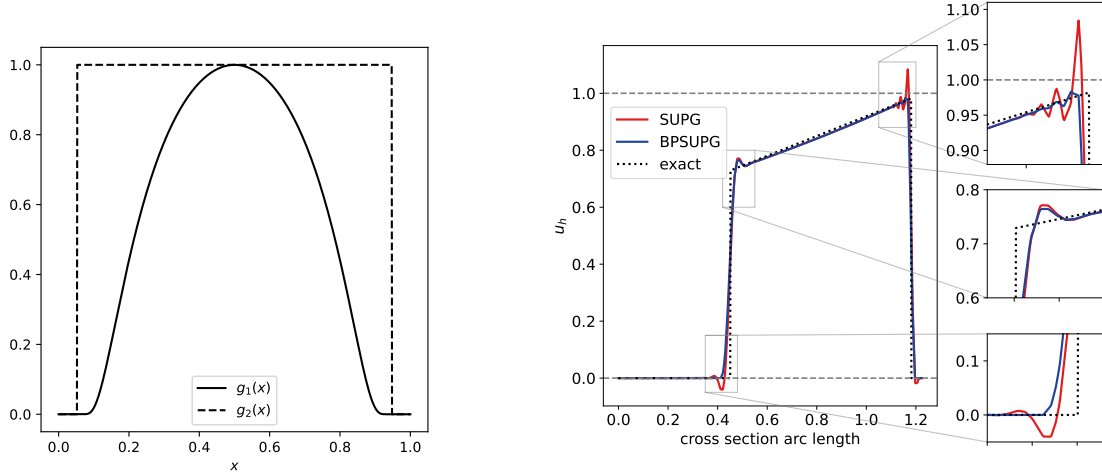
6.2. Example 2: linear reaction with discontinuous boundary data. We now consider a more challenging variation on Example 1 where the boundary condition is discontinuous:

$$(78) \quad g_2(x, y) := \begin{cases} 1 & \text{if } |x - \frac{1}{2}| < \frac{1}{\sqrt{5}}, \\ 0 & \text{otherwise.} \end{cases}$$

A solution can still be found using the method of characteristics, but this solution inherits the discontinuity as it is propagated along the characteristics from the inflow boundary. We will therefore not have the necessary regularity on the solution for error estimates given in 3.5 to hold, since the interpolation estimates are too limited by the lack of regularity - indeed in light of Remark 2.2, we only expect the solution to lie in the graph space. The particular challenge of this example is the spurious oscillations which are expected to be exacerbated by the discontinuity. The exact solution is given by

$$(79) \quad u_2(x, y) = \begin{cases} \exp\left(-\frac{y}{\sqrt{2}}\right) & \text{if } -\sqrt{\frac{2}{5}} < y - x\sqrt{2} + \frac{1}{\sqrt{2}} < \sqrt{\frac{2}{5}}, \\ 0 & \text{otherwise.} \end{cases}$$

In Figure 1b we display convergence rates for the bound-preserving finite element method, and in Figure 3b a comparison with the standard SUPG case without enforcing bounds is presented. As expected, we do not obtain the desired convergence rate, but a stable solution is obtained, with much reduced numerical artefacts, as seen in Figure 3b.



(A) An illustration of the boundary conditions g_1 and g_2 chosen for Examples 1 & 2.

(B) Cross section of exact and numerical solutions along the line perpendicular to the wind field \mathbf{b}_1 and passing through the point $(1, 0)$.

FIGURE 3. Note that the standard SUPG solution exhibits oscillations which cause the violation of the analytical bounds on the solution, and that this issue is remedied by the use of the bound-preserving method.

6.3. Example 3: A discontinuous pure advection problem. To demonstrate the effectiveness of the bound preserving method for a problem with low regularity and where violation of the maximum principle is expected when standard finite element methods are used, we consider a pure advection problem with discontinuous data on the inflow boundary. Numerical solutions to such problems typically suffer from spurious under- and over-shoots as the discontinuity is propagated by the velocity field. The advection field is chosen to be

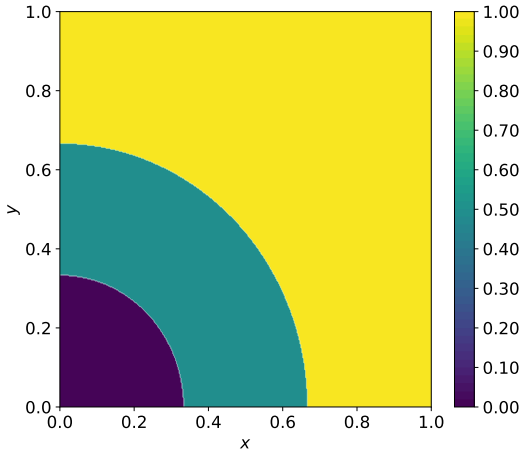
$$(80) \quad \mathbf{b}_3(x, y) := \frac{1}{\sqrt{x^2 + y^2}}(-y, x),$$

so that the inflow boundary is in this case defined by

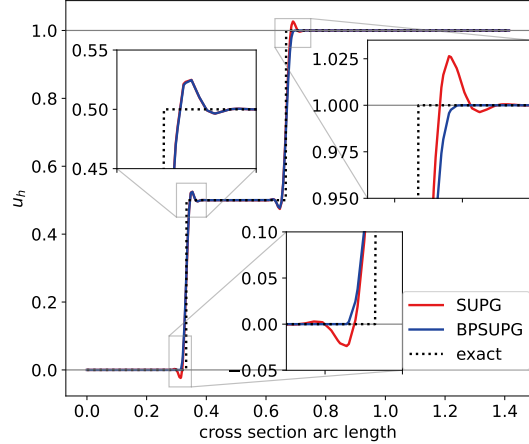
$$\Gamma^+ = \{(x, y) \in \partial\Omega : x = 1\} \cup \{(x, y) \in \partial\Omega : y = 0\}.$$

Boundary data is prescribed as follows:

$$(81) \quad g_3(x, y) := \begin{cases} 0 & \text{if } x < \frac{1}{3}, \\ \frac{1}{2} & \text{if } \frac{1}{3} \leq x < \frac{2}{3}, \\ 1 & \text{otherwise,} \end{cases}$$



(A) Visualisation of the piecewise constant exact solution to Example 3.



(B) Cross section of exact and numerical solutions along the line $y = x$.

FIGURE 4. Visualisations of exact and numerical solutions to Example 3, §6.3. The numerical solution obtained from the variational inequality problem and discretised with BPSUPG using \mathbb{P}_1 elements, $h = 2^{-7}$, is shown in blue, while the regular SUPG finite element solution with the same discretisation parameters is shown in red. The dotted line is the exact solution, and grey horizontal lines indicate bounds on the exact solution which are known a priori.

resulting in a discontinuous piecewise constant solution having $H_-(\Omega)$ regularity but no better, illustrated in Figure 4a. Numerical results are shown in Figure 4, which demonstrate both the strength and weakness of this method. Indeed, the bound-preserving SUPG method (BPSUPG) satisfies the bound $u_h(\mathbf{x}) \in [0, 1] \forall \mathbf{x} \in \Omega$, and the oscillations that occur near $u_h = 0$ and $u_h = 1$ are completely removed (see Figure 4b), but oscillations which lie away from the minimum and maximum values are not alleviated by the method.

6.4. Example 4: nonlinear reaction with smooth boundary data. We now consider the following problem

$$(82) \quad \begin{aligned} \mathbf{b} \cdot \nabla u + c|u|^{-\frac{1}{2}}u &= 0 & \text{in } \Omega \\ u &= g & \text{on } \Gamma_-, \end{aligned}$$

which we can consider as a re-scaling of Equation (35). We note that an exact solution for this problem can be found using the method of characteristics as long as \mathbf{b} is sufficiently well-behaved. Indeed, assuming that the boundary data is non-negative, we consider the behaviour of u along a characteristic which originates at \mathbf{x}_0 on Γ_- . Then if the characteristic containing \mathbf{x}_0 is parameterised by t , we have

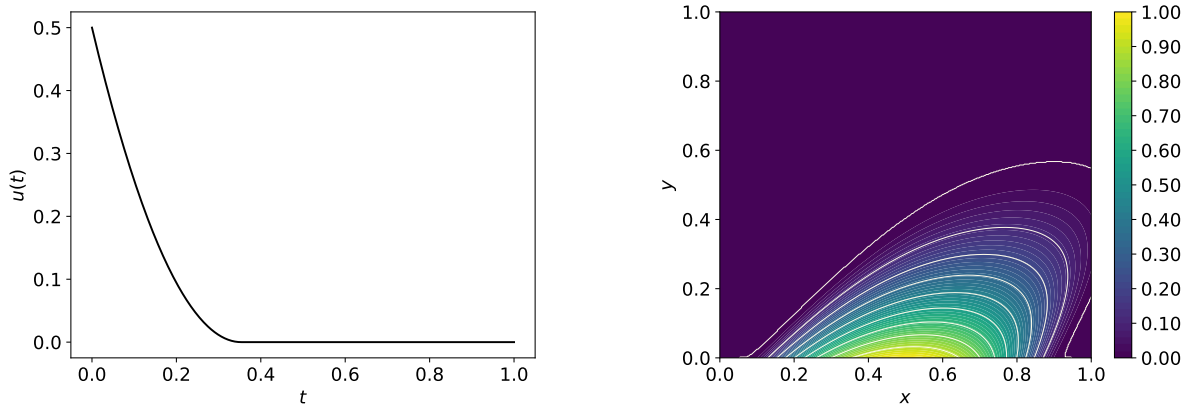
$$(83) \quad \frac{d}{dt}u(\mathbf{x}(t)) + c|u|^{-\frac{1}{2}}u = 0.$$

This ordinary differential equation is well-posed for all initial conditions u_0 , with solution given by (see also Figure 5a)

$$(84) \quad u(\mathbf{x}(t)) = \text{sgn}(u_0) \left(\max \left\{ 0, \sqrt{|u_0|} - \frac{ct}{2} \right\} \right)^2.$$

Thus, the solution approaches zero quadratically for $t < 2\sqrt{|u_0|}/c$ and is zero for all $t \geq 2\sqrt{|u_0|}/c$.

Along a characteristic, the exact solution is quadratic until it reaches zero in finite time given by $2\sqrt{|u_0|}/c$ and remains zero thereafter. It is therefore continuously differentiable, but with a second (weak) derivative



(A) Solution to Equation 83 with $u_0 = 1/2$ and $c = 4$.

(B) Contour plot of exact solution for Example 4.

FIGURE 5. Visualisations of the exact solution to Example 4, given by Equation 85.

which is discontinuous. If $u_0 = 0$, the solution is trivial. Following these observations, we deduce that if the boundary data is bounded in $[0, 1]$, then the solution u of Equation 82 satisfies the same bounds.

The inflow boundary data is set to be g_1 , with \mathbf{b}_1 again chosen for the advection field. It follows from the computation of the characteristics defined by \mathbf{b} together with the Equation 84 that the exact solution to this problem is given by

$$(85) \quad u_3(x, y) = \begin{cases} \left(\max \left\{ 0, \sqrt{g_1 \left(x - \frac{y}{\sqrt{2}}, y \right)} - c \frac{y}{2\sqrt{2}} \right\} \right)^2 & \text{if } -\sqrt{\frac{2}{5}} < y - x\sqrt{2} + \frac{1}{\sqrt{2}} < \sqrt{\frac{2}{5}}, \\ 0 & \text{otherwise.} \end{cases}$$

Since g_1 is smooth, the above observations imply that $u_3 \in H^2(\Omega)$. A visualisation of the exact solution given in Equation 85 is provided in Figure 5b.

The reduced-space active set method is again used to solve the discrete variational inequality, but this time an approximate Jacobian is used in the solve step, Equation (74), to avoid the singularity in the reaction coefficient. Since the Jacobian is singular around $u = 0$, a small amount of regularisation was added and observed to improve solver performance.

In Figure 7a we display convergence rates for the bound-preserving finite element method. As long as the SUPG parameters are chosen to be of the appropriate order, $\mathcal{O}(h^{3/2})$ convergence is obtained.

6.5. Example 5: nonlinear reaction with discontinuous boundary data. We test the nonlinear case with boundary data g_2 and advection field \mathbf{b}_1 . As above, an exact solution can be derived for this problem, however with discontinuous boundary condition, the resulting solution has minimal regularity. Convergence rates are shown in Figure 7b, again affected by the lack of regularity of the exact solution in this case. A comparison of exact and numerical solutions is given in Figure 6

7. CONCLUSIONS AND FURTHER WORK

In this work, we introduced a method for preserving bounds on numerical solutions to partial differential equations by reformulating the standard discrete weak form as a discrete variational inequality. The finite element method was analysed for both a linear first-order problem and a first-order problem with a nonlinear reaction term. The SUPG method was adapted to this bound-preserving framework, and the expected convergence rates were successfully retained.

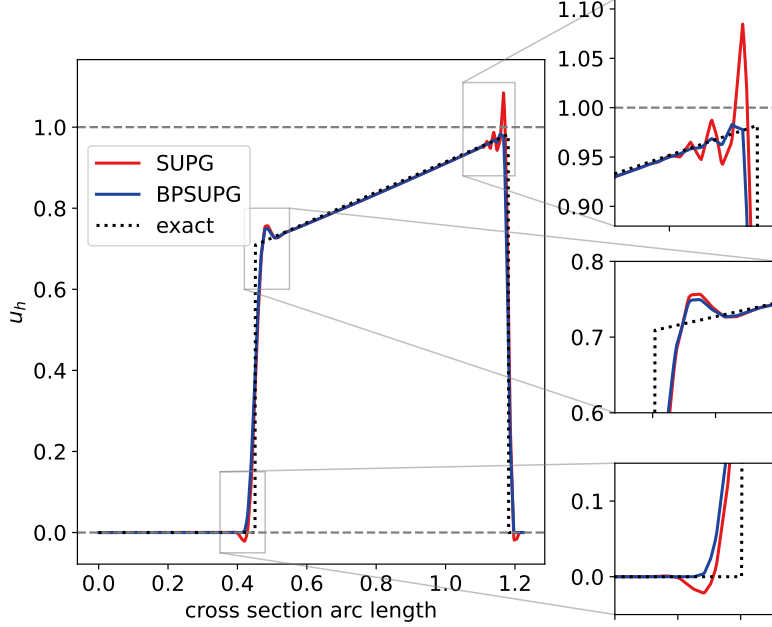
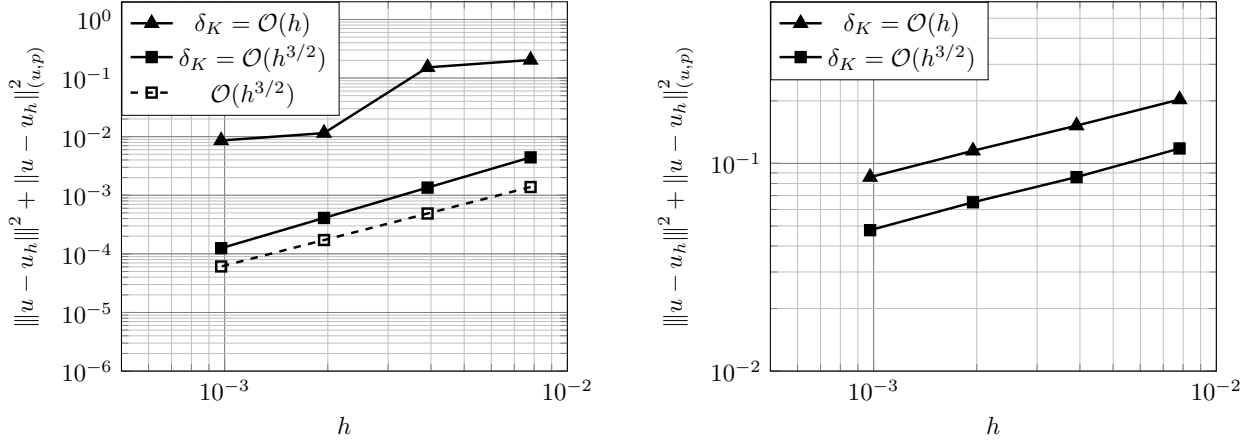


FIGURE 6. Cross section of exact and numerical solutions along the line perpendicular to the wind field \mathbf{b}_1 and passing through the point $(1, 0)$.



(A) Approximation error for Example 4 §6.4, solution in $H^2(\Omega)$.

(B) Approximation error for Example 5 §6.5, solution in $u \in H_-(\Omega) \setminus H^1(\Omega)$ only.

FIGURE 7. Approximation errors for the bound-preserving finite element method in the full SUPG + quasi norm. The choice of SUPG parameters greatly affects the performance of the method.

While certain aspects of the analysis are tailored to the specific problems considered, the proposed framework is broadly applicable and can, in principle, be extended to any problem admitting a variational formulation. This flexibility enables the application of the method to a wide range of partial differential equations using existing finite element techniques.

The approach outlined here shows particular promise for problems involving singular coefficients or where strict preservation of bounds is essential to ensure physical validity. Future work will explore the extension of this framework to kinetic equations [ACH⁺24, PPT24], where ensuring positivity of solutions is important

physically, and to models of non-Newtonian fluids [AP25], which feature complex nonlinearities and require positive preserving schemes to ensure well-posedness. Key to all these applications is the efficient solution and computational scalability of this class of method.

REFERENCES

- [ABP24] A. Amiri, G.R. Barrenechea, and T. Pryer. A nodally bound-preserving finite element method for reaction–convection–diffusion equations. *Mathematical Models and Methods in Applied Sciences*, 34(08):1533–1565, 2024.
- [ACH⁺24] B.S. Ashby, V. Chronholm, D.K. Hajnal, A. Lukyanov, K. MacKenzie, A. Pim, and T. Pryer. Efficient proton transport modelling for proton beam therapy and biological quantification. *arXiv preprint arXiv:2411.16735*, 2024.
- [Alf94] N. Alfredo. An iterative algorithm for the variational inequality problem. *Computational and Applied Mathematics*, 13:103–114, 1994.
- [AP25] B.S. Ashby and T. Pryer. Discretisation of an Oldroyd-B viscoelastic fluid flow using a lie derivative formulation. *Advances in Computational Mathematics*, 51(1):1, 2025.
- [BE05] E. Burman and A. Ern. Stabilized Galerkin approximation of convection-diffusion-reaction equations: discrete maximum principle and convergence. *Math. Comp.*, 74(252):1637–1652 (electronic), 2005.
- [Ber12] J.M. Bernard. Steady transport equation in the case where the normal component of the velocity does not vanish on the boundary. *SIAM Journal on Mathematical Analysis*, 44(2):993–1018, 2012.
- [BGMS98] S. Balay, W. Gropp, L.C. McInnes, and B.F. Smith. PETSC, the portable, extensible toolkit for scientific computation. *Argonne National Laboratory*, 2(17), 1998.
- [BGPV24] G.R. Barrenechea, E.H. Georgoulis, T. Pryer, and A. Veiser. A nodally bound-preserving finite element method. *IMA Journal of Numerical Analysis*, 44(4):2198–2219, 2024.
- [BH82] A.N. Brooks and T.J.R. Hughes. Streamline upwind/Petrov-Galerkin formulations for convection dominated flows with particular emphasis on the incompressible Navier-Stokes equations. *Computer methods in applied mechanics and engineering*, 32(1-3):199–259, 1982.
- [BHR77] F. Brezzi, W.W. Hager, and P.A. Raviart. Error estimates for the finite element solution of variational inequalities: Part i. primal theory. *Numerische Mathematik*, 28(4):431–443, 1977.
- [BJK17] G.R. Barrenechea, V. John, and P. Knobloch. An algebraic flux correction scheme satisfying the discrete maximum principle and linearity preservation on general meshes. *Math. Models Methods Appl. Sci.*, 27(3):525–548, 2017.
- [BJK23] G.R. Barrenechea, V. John, and P. Knobloch. Finite element methods respecting the discrete maximum principle for convection-diffusion equations. *SIAM Review*, 2023. to appear.
- [BL93] J.W. Barrett and W.B. Liu. Finite element approximation of the p -laplacian. *Mathematics of computation*, 61(204):523–537, 1993.
- [BM06] S.J. Benson and T.S. Munson. Flexible complementarity solvers for large-scale applications. *Optimization Methods and Software*, 21(1):155–168, 2006.
- [BPT24] G.R. Barrenechea, T. Pryer, and A. Trenam. A nodally bound-preserving discontinuous galerkin method for the drift-diffusion equation. *arXiv preprint arXiv:2410.05040*, 2024.
- [CEL⁺24] A. Callo, M. Evans, H. Lockyer, F. Madiot, T. Pryer, and L. Zanetti. Cycle-free polytopal mesh sweeping for Boltzmann transport. *arXiv preprint arXiv:2412.01660*, 2024.
- [CJ21] E. Celledoni and J. Jackaman. Discrete conservation laws for finite element discretisations of multisymplectic pdes. *Journal of Computational Physics*, 444:110520, 2021.
- [CN17] J. Chang and K.B. Nakshatrala. Variational inequality approach to enforcing the non-negative constraint for advection–diffusion equations. *Computer Methods in Applied Mechanics and Engineering*, 320:287–334, 2017.
- [CR73] P.G. Ciarlet and P.A. Raviart. Maximum principle and uniform convergence for the finite element method. *Comput. Methods Appl. Mech. Engrg.*, 2:17–31, 1973.
- [EG21] A. Ern and J.L. Guermond. *Finite Elements I*. Springer, 2021.
- [Fal74] R.S. Falk. Error estimates for the approximation of a class of variational inequalities. *Mathematics of Computation*, 28(128):963–971, 1974.
- [GMP14] J. Giesselmann, C. Makridakis and T. Pryer. Energy consistent discontinuous galerkin methods for the Navier–Stokes–Korteweg system. *Mathematics of Computation*, 83(289):2071–2099, 2014.
- [GT10] V. Girault and L. Tartar. Régularité dans L^p et $W^{1,p}$ de la solution d’une équation de transport stationnaire. *Comptes rendus. Mathématique*, 348(15-16):885–890, 2010.
- [HGR08] L. Tobiska H.G. Roos, M. Stynes. *Robust Numerical Methods for Singularly Perturbed Differential Equations*. Springer Berlin, Heidelberg, 2008.
- [HKM⁺23] D.A. Ham, et. al. *Firedrake User Manual*. Imperial College London and University of Oxford and Baylor University and University of Washington, first edition edition, 5 2023.
- [JNP84] C. Johnson, U. Navert and J. Pitkaranta. Finite element methods for linear hyperbolic problems. *Computer methods in applied mechanics and engineering*, 45:285–312, 1984.
- [KS24a] B. Keith and T.M. Surowiec. Proximal Galerkin: A structure-preserving finite element method for pointwise bound constraints. *Foundations of Computational Mathematics*, pages 1–97, 2024.
- [KS24b] R.C. Kirby and D. Shapero. High-order bounds-satisfying approximation of partial differential equations via finite element variational inequalities. *Numerische Mathematik*, pages 1–21, 2024.

- [Kuz07] D. Kuzmin. Algebraic flux correction for finite element discretizations of coupled systems. In M. Papadrakakis, E. Oñate, and B. Schrefler, editors, *Proceedings of the Int. Conf. on Computational Methods for Coupled Problems in Science and Engineering*, pages 1–5. CIMNE, Barcelona, 2007.
- [Liu00] W. Liu. Finite element approximation of a nonlinear elliptic equation arising from bimaterial problems in elastic-plastic mechanics. *Numerische Mathematik*, 86:491–506, 2000.
- [MH85] A. Mizukami and T.J.R. Hughes. A Petrov-Galerkin finite element method for convection-dominated flows: an accurate upwinding technique for satisfying the maximum principle. *Comput. Methods Appl. Mech. Engrg.*, 50(2):181–193, 1985.
- [PPT24] A. Pim, T. Pryer and A. Trenam. Optimal control of a kinetic equation. *arXiv preprint arXiv:2412.10747*, 2024.
- [Rau72] J. Rauch. L2 is a continuable initial condition for Kreiss’ mixed problems. *Communications on Pure and Applied Mathematics*, 25(3):265–285, 1972.
- [RR06] M. Renardy and R.C. Rogers. *An introduction to partial differential equations*, volume 13. Springer Science & Business Media, 2006.
- [SL18] P.W. Schroeder and G. Lube. Divergence-free H(div)-fem for time-dependent incompressible flows with applications to high Reynolds number vortex dynamics. *Journal of Scientific Computing*, 75(2):830–858, 2018.
- [SP22] L.R. Scott and S. Pollock. Transport equations with inflow boundary conditions. *Partial Differential Equations and Applications*, 3(3):35, 2022.
- [WGZ22] C. Wang, Y. Guo and Z. Zhang. Unconditionally energy stable and bound-preserving schemes for phase-field surfactant model with moving contact lines. *Journal of Scientific Computing*, 92(1):20, 2022.
- [WY24] S. Wang and G. Yuan. Discrete strong extremum principles for finite element solutions of advection-diffusion problems with nonlinear corrections. *International Journal for Numerical Methods in Fluids*, 96(12):1990–2005, 2024.
- [XZ99] J. Xu and L. Zikatanov. A monotone finite element scheme for convection-diffusion equations. *Math. Comp.*, 68(228):1429–1446, 1999.
- [ZYK⁺21] Z. Zhu, H. Yang, J. Kou, T. Cheng, and S. Sun. Bound-preserving inexact Newton algorithms on parallel computers for wormhole propagation in porous media. *Computers and Geotechnics*, 138:104340, 2021.

¹ INSTITUTE FOR MATHEMATICAL INNOVATION, UNIVERSITY OF BATH, BATH, UK., ² DEPARTMENT OF MATHEMATICAL SCIENCES, UNIVERSITY OF BATH, BATH, UK.